2022 44th Annual International Conference of
the IEEE Engineering in Medicine & Biology Society (EMBC)
Scottish Event Campus, Glasgow, UK, July 11-15, 2022

2022 44th Annual International Conference of the IEEE Engineering in Medicine & Biology Society (EMBC) | 978-1-7281-2782-8/22/$31.00 ©2022 IEEE | DOI: 10.1109/EMBC48229.2022.9871582

A Comparison of Flow- and Pressure-Controlled Infusion Strategies for Microneedle-based Transdermal Drug Delivery

Ryan Sebastian, Theo Guillerm, Fjodors Tjulkins, Yuan Hu, A. James P. Clover, Alexander Lyness and Conor O'Mahony, *Senior Member, IEEE*

***Abstract*— Microneedle-based transdermal drug delivery is considered an attractive alternative to conventional injections using hypodermic needles due to its minimally invasive and painless nature; this has the potential to improve patient adherence to medication regimens. Hollow microneedles (MNs) are sharp, sub-millimeter protrusions with a channel that serves as a fluidic interface with the skin. This technology could be coupled with micro-pumps, embedded sensors, actuators and electronics to create Micro Transdermal Interface Platforms - smart, wearable infusion systems capable of delivering precise microdoses over a prolonged period. Using 500 μm tall hollow microneedles, *ex-vivo* human skin and a customized application/retraction device, this work focuses on comparing two infusion control strategies, namely 'set pressure' (SP) and 'set flow' (SF) infusion. It was found that flow-controlled infusion was capable of delivering higher volumes than pressure-driven delivery, and a mean volume of 3.8 mL was delivered using a set flowrate of 50 μL/minute. This suggests that flow driven delivery is a better control strategy and confirms that MN array retraction is beneficial for transdermal MN infusion.**

***Clinical Relevance*— This work experimentally demonstrates that flow driven infusion may be a superior control strategy for transdermal delivery using hollow microneedle arrays.**

I. Introduction

Skin is the largest organ on the human body and its outermost layer, the *stratum corneum* (SC), has excellent barrier properties which subsequently limit transdermal drug delivery through passive diffusion [1]. Microneedles (MNs) are sharp needle-like structures that are generally less than 1 millimeter in height. MNs, usually arranged in arrays, are an attractive option to overcome the barrier property of skin and, due to their short length, MN penetration is perceived as being "painless" in comparison to hypodermic needles [2]. In studies where MN penetration pain was measured on human subjects using Visual Analogue Scale, 480 μm tall MNs were perceived as eliciting less than 10% of the pain perceived due to the use of a 26 G hypodermic needle [3] and 150 μm tall needles were indistinguishable from having a flat surface pressed against the skin [4]. This substantial lack of perceived pain in comparison to hypodermic needles is a key benefit of using MNs for TDD as injection pain is a common reason for non-compliance of patients to drug treatments [5].

Many varieties of MNs exist, such as hollow, solid, coated, dissolvable and hydrogel forming needles. Solid MNs are removed after application and a drug is the applied to the surface of the skin, which diffuses through the resulting micropores at the penetration site [6]. Coated MNs use a drug formulation coated on the needle surface, which is absorbed into the skin after penetration [7]. In the case of dissolvable MNs, the drug is incorporated into the water-soluble polymer from which the structure is formed and the needle dissolves after penetration, releasing the drug [8]. Hydrogel forming microneedles, upon contact with the interstitial fluid within the epidermal layers, swell and form an unblockable conduit through which therapeutic agents and vaccines diffuse from a reservoir attached to the back of the needles into the skin [9]. Hollow MNs have a channel through which substances can pass into the skin once penetrated. Hollow microneedles are used in a manner similar to hypodermic needles, and are capable of delivering relatively large doses using a variety of infusion control techniques [10].

Hollow MNs have been used in clinical studies previously, e.g. where a study by Kochba et al. compared injections using a conventional 25G hypodermic needle with MicronJet © consisting of 450 μm tall MNs to deliver insulin to type 2 diabetes patients. It was found that MN injections resulted in a more favorable pharmacokinetic profile than subcutaneous hypodermic needle injection [11].

Previous hollow MN drug delivery studies have used either manual administration via a syringe [11], [12], or automated devices such as syringe drivers [13] and pumps [14]. Alternatively, hollow MN infusion has also been performed by maintaining a constant gas pressure on the liquid in a drug reservoir [15]. Infused volumes ranged from several hundred μL to 1 mL [13], [15].

Transdermal delivery using hollow microneedles can be achieved by controlling either the pressure or the flowrate at which the formulation is infused. During 'set pressure' (SP) administration a target pressure is maintained and the flowrate is allowed to vary in response. Conversely, during SF infusion, a target flowrate is maintained and the pressure varies. While the literature contains several instances of SP or SF infusion studies, we were unable to find any comparisons between these two control methods. The use of such control strategies will become particularly important as the development of wearable drug delivery devices accelerates. These Micro Transdermal Interface Platforms (MicroTIPs) will merge MNs with miniaturized actuators, embedded sensors and wireless

* This work was supported by Enterprise Ireland and the ECSEL Joint Undertaking under grant number H2020-ECSEL-2019-IA-876190 (Moore4Medical), by Enterprise Ireland and West Pharmaceutical Services under grant number IP2017/0560, and by the Science Foundation Ireland (SFI) Insight Centre for Data Analytics (SFI/12/RC/2289-P2)

R. Sebastian, T. Guillerm, F. Tjulkins, Y. Hu and C. O'Mahony are with the Tyndall National Institute, University College Cork, Ireland (e-mail: conor.omahony@tyndall.ie).

A. J. P. Clover is with the Dept. Plastic and Reconstructive Surgery, University College Cork, Cork, Ireland.

A. Lyness is with West Pharmaceutical Services, Exton, PA, USA.

communications to form patch-like devices. As the associated sensors, electronics and artificial intelligence will facilitate a level of closed-loop infusion control that is not currently available, it is crucial to have a deeper understanding of the mechanisms that may be used to force flow through microneedle arrays, and of how these might affect the volume and rate at which therapeutic agents might be delivered via the transdermal route [16].

Previous studies have demonstrated that MN retraction is key for successful injection. It was found that MNs cause skin compaction upon insertion, which impedes fluid flow. Additionally, the MN lumens become clogged with tissue upon insertion. Both these effects are relieved by the MN retraction [15][17].

In this paper, we investigate the delivery efficacy of a 3x1 array of 500 µm tall silicon microneedles using both set flow and set pressure strategies. An experimental setup involving *ex-vivo* human skin and periodic array retraction [17] is used to investigate the relative merits of a 50 µL/min SF protocol and a 100 kPa SP protocol. The data shows that for the parameters investigated here, SF results in significantly higher delivery volumes. Mean volume of over 3.8 mL were delivered using SF, significantly exceeding the 1.8 mL mean volume delivered using a SP approach.

II. Materials and Methods

A. Microneedle Fabrication

The hollow silicon MNs were manufactured from 100 mm diameter boron doped silicon wafers. The needle locations on the front of the wafer and the needle bore locations on the back of the wafer were defined using oxide/nitride hard masks, patterned using common photolithography techniques. Wet etching using 29% w/v KOH was carried out to define the needle structure from the front of the wafer. The wet etching formed two planes on each corner of the squares on the mask due to convex corner undercutting, which eventually intersected to form the octagonal conical structure of the MNs [18]. These needles were 500 µm tall, had tip radii of 50-100 nm and were spaced at a pitch of 1750 µm.

After forming the MN structures, a layer of aluminum was sputtered on the front surface to act as an etch stop layer when etching the needle bores. DRIE (Deep Reactive Ion Etching) from the rear of the wafer was used to form the needle bores. The dry etching tool (SPTS Technologies, Newport, UK) used SF6 and C4F8 chemistries to create bores with a nominal diameter of 50 µm, which were positioned off-centre with respect to the needle axis to preserve tip sharpness and prevent clogging with tissue during penetration. SEM images of a MN and 3 x 1 array are shown in Fig. 1.

B. Skin Preparation and Infusion Protocols

This study used *ex-vivo* human skin that was obtained following plastic surgical operations. Following protocols approved by the Clinical Research Ethics Committee of the Cork Teaching Hospitals (CREC) and informed consent from all patients, the skin was excised and stored in a freezer at -80 °C after collection. Scalpels were used to cut the samples to 35 x 35 mm^2 pieces, and the underlying adipose tissue was removed. The samples were then rehydrated using 0.1 M Phosphate Buffer Saline (Sigma-Aldrich, Massachusetts, USA) and then mounted in a custom made jig which applied strain to the skin in order to mimic its natural tension.

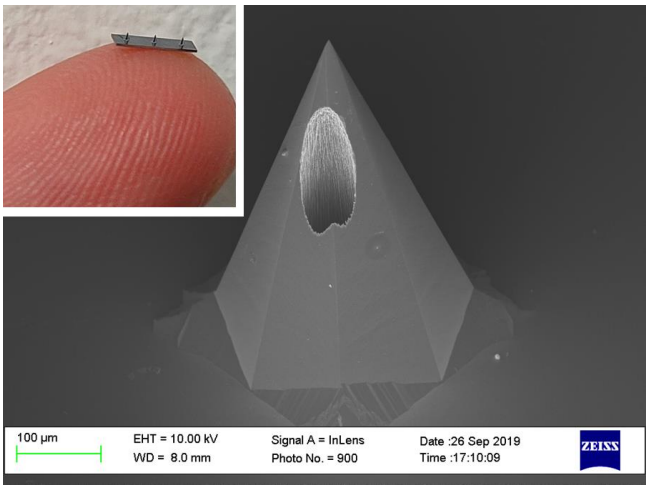

Figure 1: SEM image of a 500 µm tall hollow MN with an inset image showing a 3x1 MN array on a fingertip.

A 3 x 1 array of 500 µm tall MNs with a pitch of 1750 µm was glued to a housing to provide an interface to the fluidic circuit, which comprised an Elveflow OB1 MK3+ pressure regulator (Elvesys, Paris, France) that exerted air pressure on a reservoir of model drug consisting of aqueous methylene blue dye. Infusion pressure was measured by the regulator and flowrate was measured using an Elveflow MFS3 flow sensor.

A customized, spring-loaded applicator constructed using a modified Abeco 2006 solder removal tool (Farnell, Dublin, Ireland) with a measured spring constant of 274 N/m, was mounted on a micro-positioner system (Newport Spectra-Physics Ltd, Oxfordshire, UK). The applicator, which was calculated to have an impact energy of 2.9 J/cm^2 during skin penetration and to provide a residual compressive force of 0.274 N immediately after application, was used to apply the MN array to skin. The MN array was retracted by 100 µm using the micro-positioner every three minutes during infusion. Repeated retractions were required as the bleb expanded in response to the injected volume, which subsequently compressed against the MN base and impeded fluid flow [17]. Due to this bleb expansion, the cumulative retraction distance was often greater than the needle height, but ultimately retraction lead to leakage at which point the infusion was stopped. Leaks were detected by checking for the emergence of liquid from the interface between skin and MNs and also by observing the flow rate for large and prolonged flow. The volume infused into the skin was calculated by integrating the flowrate over time.

After infusion, the skin around the MN penetration site was cut from the initial sample using a scalpel and a further longitudinal dissection was made to expose the cross section of the infused skin. This was examined and imaged under a Stemi DV4 microscope (Zeiss, Oberkochen, Germany).

III. Results

Typical pressure and flowrate profiles resulting from SP and SF infusion are shown in Fig. 2. The retraction of MN arrays was carried out every 3 minutes during infusion, which, in most cases, resulted in a subsequent rise in flowrate for both

SP and SF. The increase in flowrate is believed to be caused by reduced residual compressive force exerted on the skin following retraction and also the retraction potentially resulting in the withdrawal of any tissue that may be occluding the lumen of the MNs.

It is seen from Fig. 2A, that SP maintained the target infusion pressure of 100 kPa, resulting in flowrates of around 30 µL/min. Of note is the significant increase in flow at the point of the first retraction after three minutes. Fig. 2B shows that SF caused a large initial pressure buildup, which decayed significantly as flow through the skin became established. This suggests that in order to maintain a set infusion flowrate, the capability to generate high pressure is required at the start of the infusion and then a much lower pressure can be used. Gupta et al. [13] indicated that injection flowrates and pressures higher than those observed in the SF test caused substantially less pain than that experienced during the insertion of a 26 G hypodermic needle. While that study also noted that MN retraction increases pain, the retraction distance and flowrates used were larger than those used here.

A sharp increase in flowrate is visible at the end of both tests, due to a leak at which point the test was ended. It is thought that this leak was due to removal of the needles from the skin when the cumulative retraction distance exceeded the height of the bleb that was formed during infusion.

9 SP and 10 SF tests were carried out, and the volumes infused are shown in Fig. 3. The mean volume infused using SP and SF were 1.75 mL and 3.80 mL respectively. This difference in mean volumes infused was found to be statistically significant using a double tailed, two sample t-test (P = 0.001, α = 0.05), which indicates that SF with a target flowrate of 50 µL/min was capable of delivering a larger volume than SP with a target pressure of 100 kPa. This suggests that SF is likely to be a better control strategy for MN infusion in terms of delivering larger volumes. In addition, a control strategy based on flowrate allows the infusion to be directly controlled to deliver a certain dosage in a certain time frame as the target flowrate is easily calculated from the desired delivery volume.

A representative image of the skin after infusion, with the MNs removed, is shown in Fig. 4. Methylene blue dye is clearly evident below the surface of the skin, and droplets of dye are seen to be emerging from the MN entry site (Fig. 4A). This is believed to be caused by the pressure of the bolus inside the skin driving the fluid outwards in the absence of the MN array and/or the residual compressive force provided by the MN application. Fig. 4B shows the cross section of the skin post infusion. The presence of the dye is seen clearly throughout the skin, confirming delivery of the model drug.

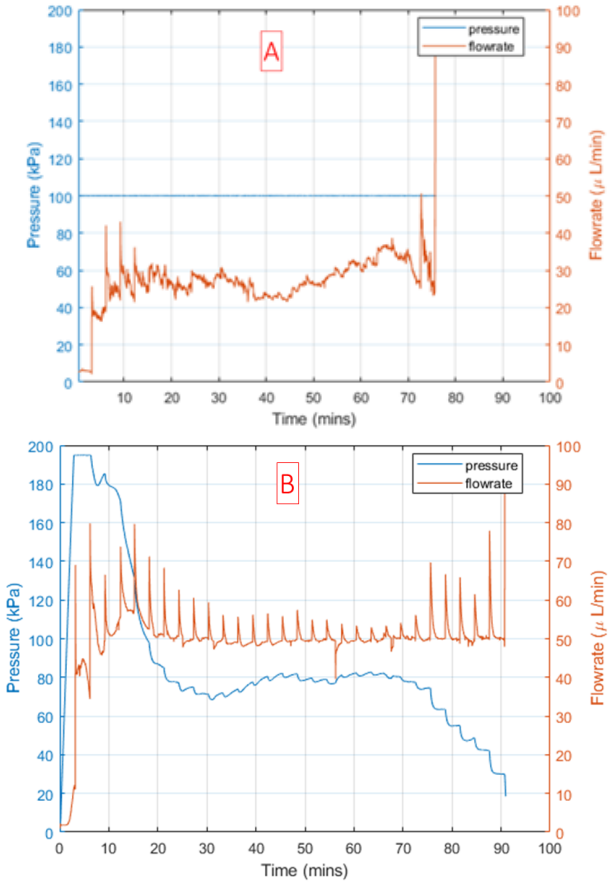

Figure 2: Pressure and flowrate vs. time for a typical SP (A) and SF (B) test. The target pressure for SP was 100 kPa and the target SF flowrate was 50 µL/min. MN array retractions were performed every 3 minutes, which on most occasions results in a subsequent rise in flowrate for both SP and SF. Note the spike in flowrate at the end of both tests is as a result of the leak which caused the test to end.

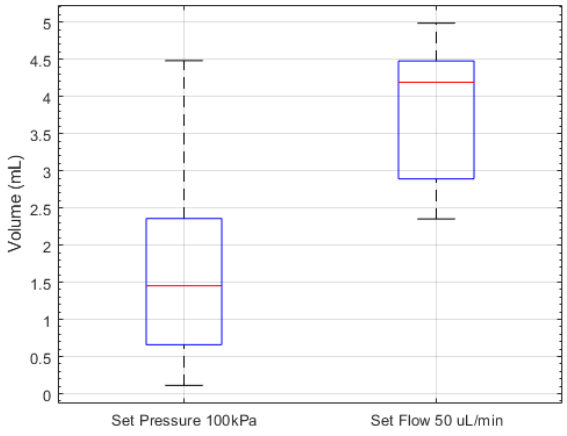

Figure 3: Comparison of volumes delivered using SP (n=9) and SF (n=10). The mean infused volumes using SP and SF were 1.75 mL and 3.80 mL respectively. The difference between these means were found to be statistically significant (P = 0.001, α = 0.05), meaning that SF with a target flowrate of 50 µL/min is capable of delivering a larger volume than SP with a target pressure of 100 kPa.

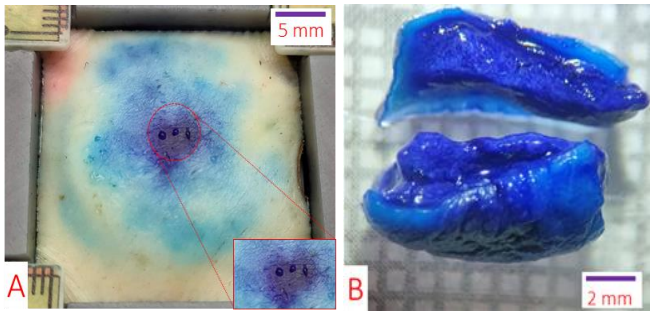

Figure 4: A) Post infusion image of the skin sample on the jig. Methylene blue dye is seen under the surface of the skin as a result of infusion. The inset image shows a close up view of the delivery site where the pressure of the delivered bolus within the skin is forcing the methylene blue droplets to be slowly expelled through the MN penetration sites. B) Cross section of the delivery site showing clear evidence of methylene blue delivery.

A possible shortcoming of the *ex-vivo* tissue model used here and in other works is that it does not account for the additional fluidic resistance that may be provided by underlying adipose and skeletal muscle tissue. We suspect that for injections performed on *in-vivo* skin, the fluidic resistance could be higher due to the presence of underlying tissue and therefore a greater pressure may be required to maintain long-term infusion. This creates scope for further investigation using *in-vivo* models. It is also noted that this work used just a single parameter – estimated from values commonly seen in the literature - for each of the SP and SF delivery protocols. Further investigation, based on the methods outlined here, and involving a more extensive matrix of SP, SF and retraction parameters is warranted to more accurately determine the best infusion strategy.

IV. Conclusions

This study used an *ex-vivo* human skin model to investigate transdermal drug delivery via hollow silicon microneedles. Two delivery control strategies were examined, namely the use of either set flow (50 µL/min) or set pressure (100 kPa) to drive fluidic infusion. It was found that once a high initial pressure was provided, SF was capable of delivering larger volumes than SP (mean volume of 3.8 mL and 1.8 mL, respectively), which suggests that SF may be a better infusion control strategy for MN-based drug delivery systems. As reported elsewhere, periodic retraction of the MNs during infusion was also key to establishing and maintaining flow.

The data highlights that significant variations in delivery volumes may arise as a result of differing infusion strategies. This study also underlines the importance of attaining a deeper understanding of microneedle-based delivery mechanisms in order to take full advantage of the opportunities that will be provided by the closed-loop sensor/actuator control incorporated in emerging wearable systems such as Micro Transdermal Interface Platforms (MicroTIPs).

Acknowledgment

The authors thank Tyndall's Specialty Products and Services team for microneedle processing.

References

[1] C. M. Schoellhammer, D. Blankschtein, and R. Langer, "Skin permeabilization for transdermal drug delivery: recent advances and future prospects," *Expert Opin. Drug Deliv.*, vol. 11, no. 3, pp. 393–407, Mar. 2014, doi: 10.1517/17425247.2014.875528.

[2] M. R. Prausnitz, "Microneedles for transdermal drug delivery," *Adv. Drug Deliv. Rev.*, vol. 56, no. 5, pp. 581–587, Mar. 2004, doi: 10.1016/j.addr.2003.10.023.

[3] H. S. Gill, D. D. Denson, B. A. Burris, and M. R. Prausnitz, "Effect of Microneedle Design on Pain in Human Volunteers," *Clin. J. Pain*, vol. 24, no. 7, pp. 585–594, Sep. 2008, doi: 10.1097/AJP.0b013e31816778f9.

[4] S. Kaushik *et al.*, "Lack of Pain Associated with Microfabricated Microneedles," *Anesth. Analg.*, vol. 92, no. 2, pp. 502–504, Feb. 2001, doi: 10.1213/00000539-200102000-00041.

[5] M. Peyrot, A. H. Barnett, L. F. Meneghini, and P.-M. Schumm-Draeger, "Factors associated with injection omission/non-adherence in the Global Attitudes of Patients and Physicians in Insulin Therapy study," *Diabetes, Obes. Metab.*, vol. 14, no. 12, pp. 1081–1087, Dec. 2012, doi: 10.1111/j.1463-1326.2012.01636.x.

[6] L. Wei-Ze *et al.*, "Super-short solid silicon microneedles for transdermal drug delivery applications," *Int. J. Pharm.*, vol. 389, no. 1–2, pp. 122–129, Apr. 2010, doi: 10.1016/j.ijpharm.2010.01.024.

[7] L. Liang *et al.*, "Optimization of dip-coating methods for the fabrication of coated microneedles for drug delivery," *J. Drug Deliv. Sci. Technol.*, vol. 55, p. 101464, Feb. 2020, doi: 10.1016/j.jddst.2019.101464.

[8] J. W. Lee, J.-H. Park, and M. R. Prausnitz, "Dissolving microneedles for transdermal drug delivery," *Biomaterials*, vol. 29, no. 13, pp. 2113–2124, May 2008, doi: 10.1016/j.biomaterials.2007.12.048.

[9] R. F. Donnelly *et al.*, "Hydrogel-Forming Microneedle Arrays for Enhanced Transdermal Drug Delivery," *Adv. Funct. Mater.*, vol. 22, no. 23, pp. 4879–4890, Dec. 2012, doi: 10.1002/adfm.201200864.

[10] Á. Cárcamo-Martínez, B. Mallon, J. Domínguez-Robles, L. K. Vora, Q. K. Anjani, and R. F. Donnelly, "Hollow microneedles: A perspective in biomedical applications," *Int. J. Pharm.*, vol. 599, p. 120455, Apr. 2021, doi: 10.1016/j.ijpharm.2021.120455.

[11] E. Kochba, Y. Levin, I. Raz, and A. Cahn, "Improved Insulin Pharmacokinetics Using a Novel Microneedle Device for Intradermal Delivery in Patients with Type 2 Diabetes," *Diabetes Technol. Ther.*, vol. 18, no. 9, pp. 525–531, Sep. 2016, doi: 10.1089/dia.2016.0156.

[12] Y. Levin, E. Kochba, I. Hung, and R. Kenney, "Intradermal vaccination using the novel microneedle device MicronJet600: Past, present, and future," *Hum. Vaccin. Immunother.*, vol. 11, no. 4, pp. 991–997, Apr. 2015, doi: 10.1080/21645515.2015.1010871.

[13] J. Gupta, S. S. Park, B. Bondy, E. I. Felner, and M. R. Prausnitz, "Infusion pressure and pain during microneedle injection into skin of human subjects," *Biomaterials*, vol. 32, no. 28, pp. 6823–6831, Oct. 2011, doi: 10.1016/j.biomaterials.2011.05.061.

[14] E. McVey, S. Keith, J. K. Herr, D. Sutter, and R. J. Pettis, "Evaluation of Intradermal and Subcutaneous Infusion Set Performance Under 24-Hour Basal and Bolus Conditions," *J. Diabetes Sci. Technol.*, vol. 9, no. 6, pp. 1282–1291, Nov. 2015, doi: 10.1177/1932296815598327.

[15] W. Martanto *et al.*, "Microinfusion Using Hollow Microneedles," *Pharm. Res.*, vol. 23, no. 1, pp. 104–113, Jan. 2006, doi: 10.1007/s11095-005-8498-8.

[16] C. O'Mahony *et al.*, "Embedded sensors for Micro Transdermal Interface Platforms (MicroTIPs)," in *2016 Symposium on Design, Test, Integration and Packaging of MEMS/MOEMS (DTIP)*, May 2016, pp. 1–5. doi: 10.1109/DTIP.2016.7514859.

[17] P. Shrestha and B. Stoeber, "Imaging fluid injections into soft biological tissue to extract permeability model parameters," *Phys. Fluids*, vol. 32, no. 1, p. 011905, Jan. 2020, doi: 10.1063/1.5131488.

[18] N. Wilke and A. Morrissey, "Silicon microneedle formation using modified mask designs based on convex corner undercut," *J. Micromechanics Microengineering*, vol. 17, no. 2, pp. 238–244, Feb. 2007, doi: 10.1088/0960-1317/17/2/008.